Open access • Journal Article • DOI:10.1016/J.APCATB.2007.01.004

Efficient destruction of pathogenic bacteria with AgBr/TiO2 under visible light irradiation — Source link

Yongqing Lan, Chun Hu, Xuexiang Hu, Jiuhui Qu

Institutions: Chinese Academy of Sciences

Published on: 11 May 2007 - Applied Catalysis B-environmental (Elsevier)

Available online at www.sciencedirect.com
ScienceDirect
Applied Catalysis B: Environmental 73 (2007) 354–360
APPLIED CATALYSIS B: ENVIRONMENTAL
www.elsevier.com/locate/apcatb

Efficient destruction of pathogenic bacteria with AgBr/TiO_2 under visible light irradiation

Yongqing Lan, Chun Hu *, Xuexiang Hu, Jiuhui Qu

State Key Laboratory of Environmental Aquatic Chemistry, Research Center for Eco-Environmental Sciences, Chinese Academy of Sciences, Beijing 100085, China

Received 20 February 2006; received in revised form 14 December 2006; accepted 5 January 2007
Available online 13 January 2007

Abstract

The photocatalytic inactivation of pathogenic bacteria in water was investigated systematically with AgBr/TiO_2 under visible light ($\lambda > 420$ nm) irradiation. The catalyst was found to be highly effective for the killing of *Escherichia coli*, a Gram-negative bacterium, and *Staphylococcus aureus*, a Gram-positive bacterium. The decomposition of the cell wall and cell membrane was directly observed by TEM and further confirmed by K^+ leakage from the inactivated bacteria. A possible cell damage mechanism by visible light-driven AgBr/TiO_2 is proposed. In addition, the effects of pH, inorganic ions on bacterial photocatalytic inactivation were investigated. The electrostatic force interaction of the bacteria–catalyst is crucial for the efficiency of disinfection. Moreover, AgBr/TiO_2 supported on porous nickel showed much higher bactericidal activity than fixed P25 TiO_2 under visible or near UV light irradiation.

Keywords: Bactericidal mechanism; Interaction of bacteria–catalyst; Pathogenic bacteria; Visible light-driven

1. Introduction

Traditional disinfection methods, such as chlorination, ozone and chlorine dioxide, effectively kill harmful microorganisms, but afterwards, harmful disinfection by-products (DBPs) are formed. Pathogenic organisms pose the primary human health risk from drinking water, while chemical DBPs also are an unintended health hazard [1]. Therefore, the development of more effective sterilization techniques has become an urgent issue.

In 1985, Matsunaga et al. reported for the first time that TiO_2 photocatalyst could kill bacterial cells in water [2]. Since then, numerous studies related to the bactericidal effect of TiO_2 photocatalyst have been conducted to inactivate bacteria, viruses, and cancer cells [3–7]. TiO_2 photocatalytic disinfection seems to be a promising technique. However, the main drawbacks of low quantum yields and the lack of visible light utilization hinder its practical application. To address these problems, numerous studies have been performed recently to enhance the photocatalytic efficiency and visible light utilization of TiO_2; these include impurity doping [8–10], metallization [11–13], and sensitization [14,15]. The results suggest that the development of better visible light photocatalysts depends on the visible light photoresponse and highly effective interfacial charge-transfer.

Silver halides are well known as photosensitive materials and are widely employed as source materials in photographic films. Recently, a silver bromide emulsion dispersed on silica support has been studied in the CH_3OH/H_2O solution for H_2 evolution under UV illumination [16]. Also, AgBr dispersed on Al-MCM-41 showed high visible light activity for the decomposition of acetaldehyde in gas phase [17]. In a previous study, we reported the preparation and the activity and stability mechanism of AgBr/TiO_2 for the destruction of azo dyes and *Escherichia coli* [18]. These studies suggested that silver halides could act as a good visible light photocatalyst candidate for the removal of pollutants when suitable environmental conditions could be chosen to prevent their photodecomposition.

In the present study, the mechanism and kinetics of the photocatalytic destruction of pathogenic bacteria in AgBr/TiO_2 aqueous suspensions under visible light irradiation was studied

* Corresponding author. Tel.: +86 10 62849628; fax: +86 10 62923543.
E-mail addresses: huchun@rcees.ac.cn, huchun@mail.rcees.ac.cn (C. Hu).

0926-3373/$ – see front matter © 2007 Elsevier B.V. All rights reserved.
doi:10.1016/j.apcatb.2007.01.004

in detail. The interaction of bacteria–catalysts was illustrated and discussed.

2. Experimental details

2.1. Chemicals

Titania P25 (TiO_2; ca. 80% anatase, 20% rutile; BET area, ca. 50 $m^2\ g^{-1}$) was purchased from Degussa Co. *Escherichia coli* (*E. coli* DH 4α) and *Staphylococcus aureus* (*S. aureus* ATCC 6538) were purchased from the Institute of Microbiology, Chinese Academy of Sciences. All other chemicals were analytical grade. Deionized and doubly distilled water was used throughout this study.

2.2. Preparation of catalysts

$AgBr/TiO_2$ was prepared by the deposition–precipitation method according to our previous report [18]. $AgBr/TiO_2$ supported on porous nickel was prepared by the following procedure. The suspensions of $AgBr/TiO_2$ homogeneously dispersed in silica sols were deposited on a round porous spumous nickel meshwork by a spin-coating method.

2.3. Characterization of catalysts

Powder X-ray diffraction of the catalysts was recorded on a Scintag-XDS-2000 diffractometer with Cu Kα radiation (λ = 1.54059 Å). UV–vis absorption spectra of the samples were recorded on a UV–vis spectrophotometer (Hitachi UV-3100) with an integrated sphere attachment. The analyzed range was 200–800 nm, and $BaSO_4$ was the reflectance standard. Determination of the concentration of H_2O_2 formed in the aqueous catalyst suspension under visible light irradiation was performed with a photometric method described in the literature [19]. The zeta potential of catalysts in KNO_3 (10^{-3} M) solution and bacteria cells in NaCl (0.1 M) solution were measured with a Zetasizer 2000 (Malvern Co., United Kingdom). Every reading of the instrument was recorded after three consistent readings had been attained.

2.4. Photocatalytic reaction procedure

Two types of bacteria, *S. aureus*, a gram-positive bacterium, and *E. coli*, a gram-negative bacterium, were used as model bacteria in this study. They were incubated in Luria–Bertani (LB) nutrient solution at 37 °C for 18 h with shaking, and then washed by centrifugation at 4000 rpm. The treated cells were then re-suspended and diluted to $\sim 2 \times 10^8$ colony-forming units (cfu/mL) with 0.9% saline. All materials used in the experiments were autoclaved at 121 °C for 25 min to ensure sterility. The diluted cell suspension and photocatalyst were added to a 100-mL beaker with a cover. The final photocatalyst concentration was adjusted to 0.2 g/L, and the final bacterial cell concentration was $\sim 2 \times 10^7$ cfu/mL. The reaction volume was 30 mL. The reaction mixture was stirred with a magnetic stirrer throughout the experiment. The light source for photocatalysis was a 350-W Xe arc lamp (Shanghai Photoelectric Devices Ltd.). Light was passed through a water filter and a UV cutoff filter (λ > 420 nm) and then was focused onto the beaker reactor. The intensity of the illumination was 2.8 mW/cm^2. The reaction temperature was maintained at 25 °C. The initial solution pH was adjusted by diluted aqueous solutions of NaOH or HCl, and the solution pH varied less than 1 pH unit throughout the reaction. A bacterial suspension without photocatalyst was irradiated as a control and the reaction mixture with no visible light irradiation was used as a dark control. Before and during the light irradiation, aliquots of the reaction solution were immediately diluted with saline and the samples with the appropriate dilution were incubated at 37 °C for 24 h on nutrient agar medium. Then the colonies were counted to determine the number of viable cells. For the measurement of K^+ leakage from the inactive bacteria, at every time interval, 1 mL of the illuminated bacterial suspension was centrifuged and the supernatant was used for inductively coupled plasma optical emission spectrometry (ICP-OES, OPTIMA 2000, Perkin Elmer Co.). All the above experiments were repeated three times.

2.5. Transmission electron microscopy (TEM)

A quantity (10^8 cfu/mL) of cells was mixed with 0.2 g/L of $AgBr/TiO_2$, and the suspensions were irradiated. At given time intervals, the cell suspensions were collected and centrifuged down to pellets. For the TEM analysis of bacteria, all samples were prepared according to the following standard procedures [20]. The bacteria pellets were pre-fixed in 2.5% glutaraldehyde at 4 °C for 12 h, and then washed two times with 0.1 M phosphate buffer (PBS) (pH 7.2). After being washed with PBS, the specimens were rendered by being mixed with 2% $Na_2H_5[P(W_2O_7)_6]$ aqueous solution at a volume ratio of 1:1 for 2 h in the dark. Then the mixing suspensions were dropped onto copper grids with holey carbon film. The grids were dried under natural conditions and examined using a TEM Hitachi H-7500. The same experiments were repeated three times.

3. Results and discussion

3.1. Characterization of catalysts

Detailed characterizations of different $AgBr/TiO_2$ were provided in our previous report [18]. Here, some major properties of the catalyst are given. The XRD patterns of $AgBr/TiO_2$ are shown in Fig. 1. In addition to the anatase and rutile phase of TiO_2, the diffraction peaks attributed to AgBr were observed. The crystallite size of AgBr was 40 nm as calculated with the Debye–Scherrer equation from the linewidth of the XRD data. The BET surface area of the sample was 22 $m^2\ g^{-1}$. As depicted in the inset of Fig. 1, the optical absorption spectra of $AgBr/TiO_2$ showed a visible light absorption band of 400–750 nm, corresponding to the indirect band gap, whereas the absorption peak around 290 nm assigned to the direct band gap of AgBr was overlaid by a strong absorption peak of TiO_2 at 277 nm.

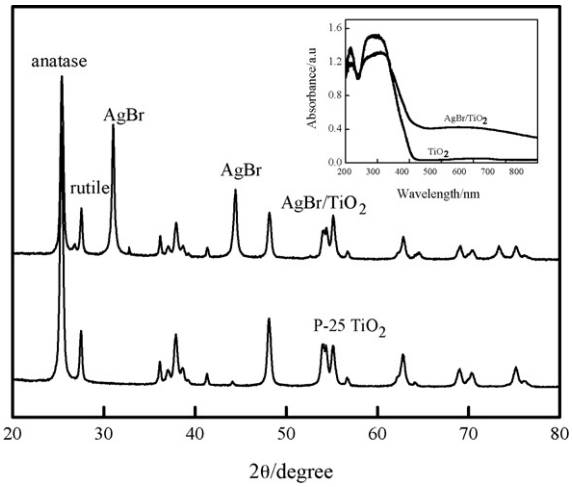

Fig. 1. XRD pattern of $AgBr/TiO_2$ and P25 TiO_2 catalysts. The inset shows UV–vis diffuse reflectance spectra of $AgBr/TiO_2$ and P25 TiO_2.

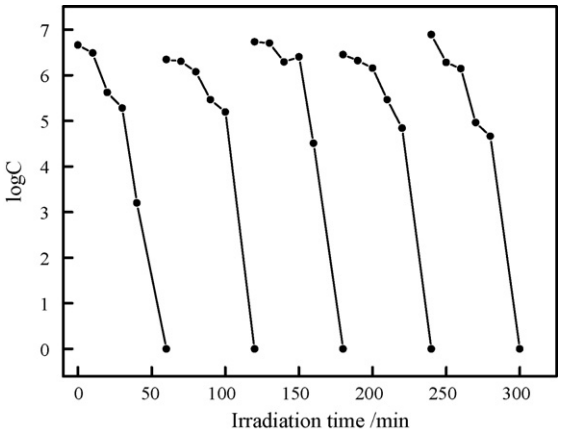

Fig. 3. Cycling runs in the photocatalytic inactivation of *E. coli* in the presence of $AgBr/TiO_2$ under visible light irradiation. $AgBr/TiO_2$ (0.2 g/L); addition of *E. coli* cells ($\sim 2 \times 10^7$ cfu/mL/run).

3.2. Photocatalytic inactivation of bacteria under visible light irradiation

The bactericidal activities of the samples were evaluated by the inactivation of *E. coli* and *S. aureus* in water under visible light irradiation. *E. coli* is a Gram-negative bacteria and *S. aureus* is a Gram-positive bacteria. Fig. 2 shows that 6.8 log *E. coli* was completely inactivated within 60 min of irradiation (curve c), whereas complete inactivation of 6.8 log *S. aureus* occurred at 40 min of irradiation. Neither pure TiO_2 with visible light nor $AgBr/TiO_2$ in the dark showed any bactericidal effects for the two bacteria (curves a and b). The results indicated that $AgBr/TiO_2$ itself was not toxic to bacteria even though Ag^0 mainly existed on the surface of the catalyst, and AgBr was the main active component of the catalyst under visible light irradiation. Different times were required for total cell inactivation of *E. coli* and *S. aureus* due to their dissimilar cell wall constituents. Gram-negative bacteria have a thin layer of peptidoglycan and a complex cell wall with two cell membranes: an outer membrane and a plasma membrane. Gram-positive bacteria have only one membrane with a relatively thick wall composed of many layers of peptidoglycan polymer. The addition of the outer membrane of Gram-negative bacteria influences the permeability of many molecules, and under certain conditions, Gram-negative bacteria are more resistant to many chemical agents than Gram-positive cells [21]. Although our previous paper reported the stability of $AgBr/TiO_2$ for the photodegradation of azo dye acid red B [18], the durability of the catalyst was also investigated in the cycling runs in photocatalytic inactivation of *E. coli*. As shown in Fig. 3, the catalyst's activity did not significantly decrease in the inactivation of *E. coli* after five successive cycles under visible light irradiation. The results were in agreement with those reported [18].

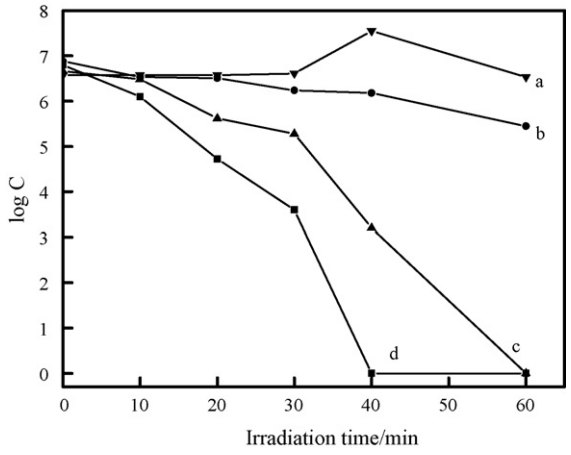

Fig. 2. Temporal course of the bacteria inactivation (2×10^7 cfu/mL, 30 mL) in aqueous dispersions containing 0.2 g/L of catalysts (a) *S. aureus*/*E. coli* + $AgBr/TiO_2$ in dark, (b) *S. aureus*/*E. coli* + TiO_2, (c) *E. coli* and (d) *S. aureus* in visible light-illuminated $AgBr/TiO_2$ suspension.

3.3. Bactericidal mechanisms

In our previous work, electron spin resonance spectra verified that $^{\bullet}OH$ and $O_2^{\bullet -}$ radicals were formed in visible light-irradiated aqueous $AgBr/TiO_2$ suspension [18]. Therefore, these oxidative radicals should be responsible for the killing of bacteria. In the present work, the formation of H_2O_2 was determined during the killing of *E. coli* in visible light-irradiated aqueous $AgBr/TiO_2$ dispersion. As shown in Fig. 4, the quantities of H_2O_2 increased with irradiation time, reaching a maximal value of 8.86×10^{-6} M at 40 min of irradiation, and then decreased continuously and finally increased again. During the photocatalytic reaction, the formed H_2O_2 was consumed by further reacting with other active species and *E. coli*. The formation and decomposition of H_2O_2 possibly occurred at the same time. Therefore, the concentration of H_2O_2 displayed disorderly change. Compared with the inactivation curve c of *E. coli* in Fig. 2, it was found that the *E. coli* inactivation rate was low; only 3.4 log *E. coli* was completely killed for 40 min before the maximum of H_2O_2 was formed. However, after that, the rate became much faster; 3.2 log *E. coli* inactivation only took 20 min. Moreover, the decomposition of H_2O_2 also was increased; its concentration decreased to

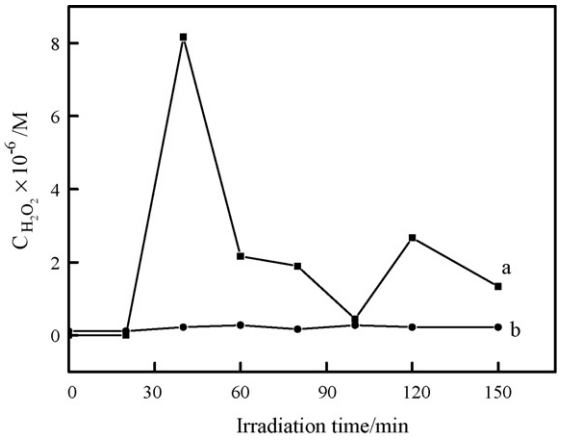

Fig. 4. Plots showing the formation of H_2O_2 in aqueous dispersions containing catalysts 3.3 g/L. (a) AgBr/TiO_2 under visible light irradiation and (b) AgBr/TiO_2 in dark.

2.1×10^{-6} M at 60 min. These results indicated that H_2O_2 rather than $^{\bullet}OH$ and $O_2^{\bullet-}$ radicals also was an active oxygen species for the killing of bacteria. To understand the bactericidal mechanism of various reactive species, the morphology of bacteria at different stages during visible light irradiation was examined by TEM. Fig. 5A–F shows the TEM images of *E. coli* and *S. aureus*, respectively. Before the photocatalytic reaction, the characteristics of the bacteria are a well-defined cell wall and an evenly rendered interior of the cell (Fig. 5A and D), corresponding to the presence of proteins and DNA. The catalyst could not enter into the cell but stayed outside of the cell wall at the starting stage of the bactericidal process. However, as irradiation time increased, great changes took place in the morphology of *E. coli* and *S. aureus* (Fig. 5B–F). Obviously, the cell wall was disrupted and the rendered interior of the cell became white, indicating that the outer membrane of the cell was damaged, leading to a leakage of the interior component. The disruption of the cell was more significant in bacterial cells treated for 120 min (Fig. 5C and F). The catalyst nanoparticles penetrated inside the cells, resulting in more damage to the membranes of the cells. TEM investigation indicated that these active species ($^{\bullet}OH$, $O_2^{\bullet-}$, H_2O_2) generated from the visible light-excited AgBr/TiO_2 could decompose the lipopolysaccharide layer and peptidoglycan layer, and subsequently destroy the cell wall and membrane, leading to leakage of the cell's intracellular substances. K^+ exists universally in bacteria [22,23] and plays a role in the regulation of polysome content and protein

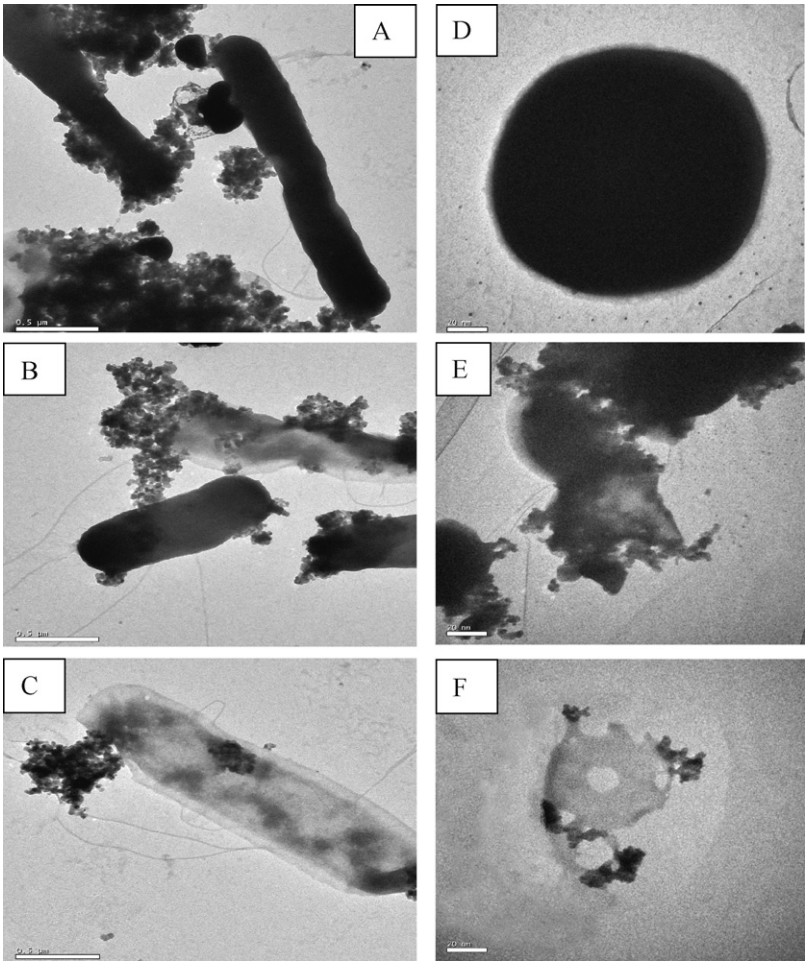

Fig. 5. TEM images of bacteria for different reaction time in visible light-illuminated AgBr/TiO_2 suspension: (A) *E. coli* before reaction, (B) *E. coli* treated for 30 min, (C) *E. coli* treated for 120 min, (D) *S. aureus* before reaction, (E) *S. aureus* treated for 30 min, and (F) *S. aureus* treated for 120 min.

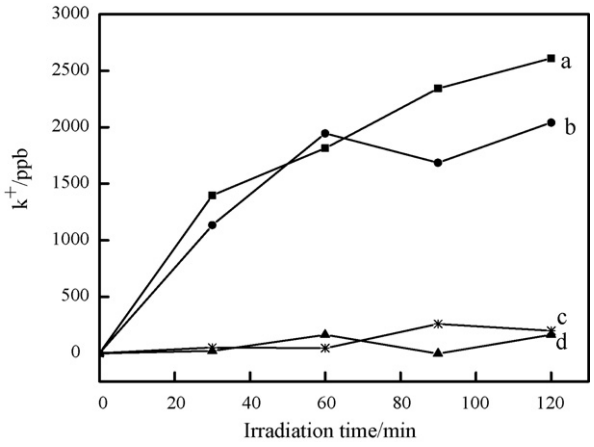

Fig. 6. Leakage of K^+ from bacterial cells in 0.2 g/L AgBr/TiO_2 suspension. (a) *S. aureus* and (b) *E. coli* under visible light irradiation, (c) *E. coli* and (d) *S. aureus* in dark.

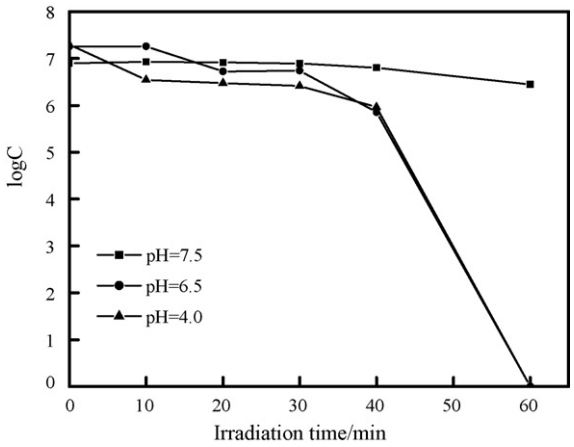

Fig. 7. The inactivation of *E. coli* ($\sim 2 \times 10^7$ cfu/mL, 30 mL) at different starting pH in visible light-irradiated AgBr/TiO_2 suspension (0.2 g/L).

synthesis. Hence, K^+ leakage was used to determine the permeability of the cell membrane. Fig. 6 shows the leakage of K^+ with inactivation of *E. coli* and *S. aureus* in AgBr/TiO_2 suspension under visible light irradiation. There was nearly no K^+ leakage from *E. coli* or *S. aureus* in the dark in the AgBr/TiO_2 system (control experiments). However, K^+ immediately leaked out from *E. coli* cells after irradiation, and its concentration increased remarkably paralleling the inactivation of bacteria with irradiation time increasing (curve b), reaching a stable value. Similarly, much higher concentrations of K^+ were released by the inactivation of the *S. aureus* cells in comparison to the K^+ concentrations from the *S. aureus* cells under the control conditions. These results implied that the visible light-induced photocatalytic reaction caused a change in the cell membrane permeability and the resultant leakage of intracellular substances, which agreed with the results of TEM measurement. These data indicate that the visible light bactericidal mechanism of AgBr/TiO_2 is similar to that of TiO_2 under UV illumination [24].

3.4. Interaction of *E. coli*–AgBr/TiO_2

3.4.1. Effect of pH on photocatalytic disinfection

Fig. 7 shows the photocatalytic inactivation of *E. coli* in irradiated AgBr/TiO_2 suspension with varying initial pHs. Clearly, the bactericidal activity of AgBr/TiO_2 decreased significantly with the pH increasing from 4.0 to 7.5. At pH 4 and pH 6.5, 7 log *E. coli* inactivation occurred at 60 min irradiation, while at pH 7.5, no significant inactivation of *E. coli* was observed. These results were predominantly attributed to the interaction of bacteria and AgBr/TiO_2. The charges of the bacteria and AgBr/TiO_2 under different pH conditions are shown in Fig. 8. In the range of pH 4–8, the overall charges of the *E. coli* cells were negative, whereas the surface of the catalyst was positively charged at pH < 4.8 which was the point of zero charge, and it was negatively charged at pH > 4.8. Electrostatic attraction existed between *E. coli* and the catalyst at pH 4, leading to more *E. coli* adsorption onto the surface of the catalyst. Thus, the catalyst exhibits more activity for the killing of *E. coli*. At pH 6.5 the surface of the catalyst was partly negatively charged because the pH was approaching the isoelectronic point (pH 4.8). The repulsive electrostatic force between *E. coli* and the catalyst was weaker, so the inactivation of *E. coli* was not significantly depressed at pH 6.5. However, at pH 7.5, the surface charge of the catalyst became more negative, and the repulsive electrostatic force was stronger. *E. coli* was not easily adsorbed on the surface of the catalyst, and the *E. coli* inactivation was nearly inhibited. Only less than 1 log *E. coli* were inactivated at 60 min of irradiation. The results indicate that interaction of AgBr/TiO_2–bacteria plays an important role in disinfection.

3.4.2. Effect of inorganic ions

To further study the effects of the interaction of the bacteria with the catalyst, inorganic ions (Ni^{2+}, Mg^{2+}, $H_2PO_4^-$, SO_4^{2-} and HCO_3^-) were added into the reaction system. As shown in Fig. 9, the inactivation rate of *E. coli* was greatly increased with the addition of Ni^{2+} and Mg^{2+} at pH 7.5 (curves e and d). 6 log *E. coli* were completely killed at 30 min of irradiation in the presence of 5 μM Ni^{2+}, and 3 log *E. coli* inactivation occurred at 60 min irradiation in the presence of 5 μM Mg^{2+}. Moreover, neither the single Ni^{2+} nor Mg^{2+} ions showed any bactericidal

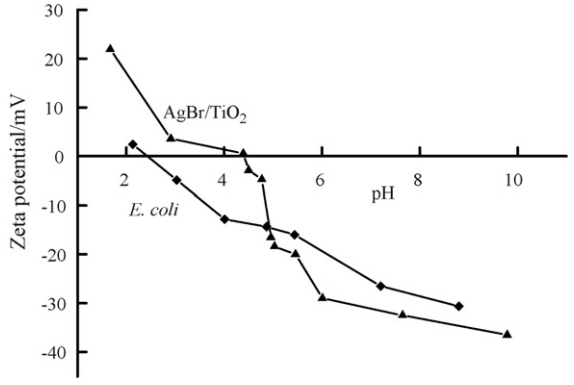

Fig. 8. Plots of the zeta potential as a function of pH for 0.1 g/L AgBr/TiO_2 suspension in the presence of KNO_3 (10^{-3} M) and *E. coli* suspension in presence of NaCl (0.1 M).

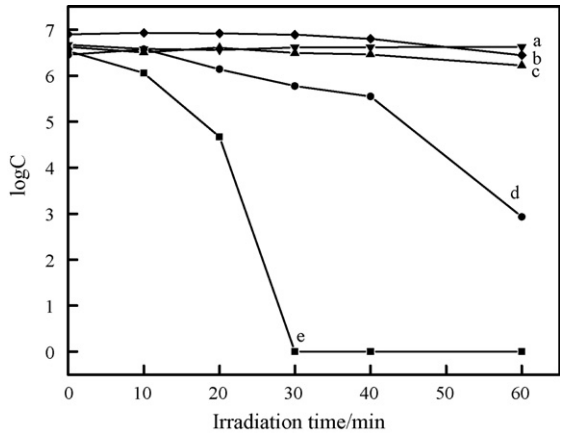

Fig. 9. Survival of *E. coli* ($\sim 2 \times 10^7$ cfu/mL, 30 mL) with visible light-irradiated AgBr/TiO_2 (0.2 g/L) dispersions at starting pH 7.5 under other wise different conditions: (a) Mg^{2+} with no catalyst, (b) Ni^{2+} with no catalyst, (c) only AgBr/TiO_2, (d) Mg^{2+}, (e) Ni^{2+}. Cations concentration: 5 μM.

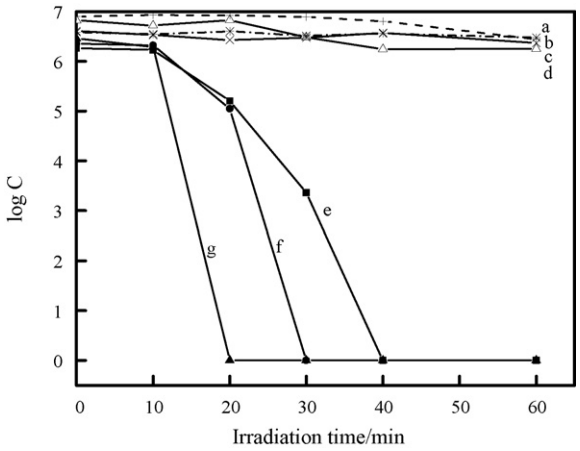

Fig. 11. Survival of *E. coli* ($\sim 2 \times 10^7$ cfu/mL, 30 mL) with visible light-irradiated AgBr/TiO_2 (0.2 g/L) dispersions at starting pH 7.5 under otherwise different conditions: (a) only AgBr/TiO_2, (b) KH_2PO_4 with no catalyst, (c) Na_2SO_4 with no catalyst, (d) $NaHCO_3$ with no catalyst, (e) KH_2PO_4, (f) Na_2SO_4, (g) $NaHCO_3$. Anions concentration: 0.1 M.

effect on *E. coli*, indicating that the tested concentration of ions did not inhibit the growth of bacteria. However, with the addition of the two ions, the zeta potential of AgBr/TiO_2 became more positive (Fig. 10) than before. Thus, at pH 7.5, the repulsive electrostatic force between *E. coli* and the catalyst was weaker than before, resulting in higher bactericidal efficiency. This result further confirmed the role of the interaction of *E. coli* and AgBr/TiO_2 in photocatalytic disinfection, although the addition of Ni^{2+} may enhance the separation of the photogenerated electrons and hole. Fig. 11 shows that, at pH 7.5, anions ($H_2PO_4^-$, SO_4^{2-} and HCO_3^-) also had positive effects on *E. coli* inactivation in AgBr/TiO_2 suspension under visible light irradiation. The single $H_2PO_4^-$ or SO_4^{2-} or HCO_3^- ions with visible light did not show any bactericidal activity, indicating that these inorganic anions themselves were not toxic to *E. coli*. Zeta potential analysis also indicated that the surface charge of AgBr/TiO_2 was not affected in the presence of anions at pH 7.5. These results suggested that mechanisms other than the interaction of *E. coli* and AgBr/TiO_2 were involved in *E. coli* inactivation. In the other experiments, it was also found that 0.1 M SO_4^{2-}, $H_2PO_4^-$ and HCO_3^- did not have any effect on the photodegradation of azo dye reactive red K-2G (K-2G) in visible light-illuminated AgBr/TiO_2 suspension. However, these ions markedly depressed the photodegradation of K-2G in AgI/TiO_2 suspension [25] under otherwise identical conditions. Only $^{\bullet}OH$ was involved in visible light-illuminated AgI/TiO_2 suspension. Since SO_4^{2-}, $H_2PO_4^-$ and HCO_3^- reacted with the holes (h_{VB}^+) and the absorbed $^{\bullet}OH$ on the surface of the catalyst to form $SO_4^{\bullet-}$, $H_2PO_4^{\bullet-}$ and $HCO_3^{\bullet-}$ [26], which were less reactive than h^+ and $^{\bullet}OH$. Their addition inhibited the activity of AgI/TiO_2 under visible light irradiation. However, in the AgBr/TiO_2 system, both $O_2^{-\bullet}$ and $^{\bullet}OH$ radicals were involved. When the $^{\bullet}OH$ radicals were scavenged by these ions, the $O_2^{\bullet-}$ radicals were still reactive oxygen species to decompose the cell wall and the cell membrane. Moreover, it has been reported that the three anions could be absorbed by *E. coli* under visible light irradiation [27]. Thus, these anion radicals would be absorbed by *E. coli* and enter into the cell, leading to strong bactericidal activity.

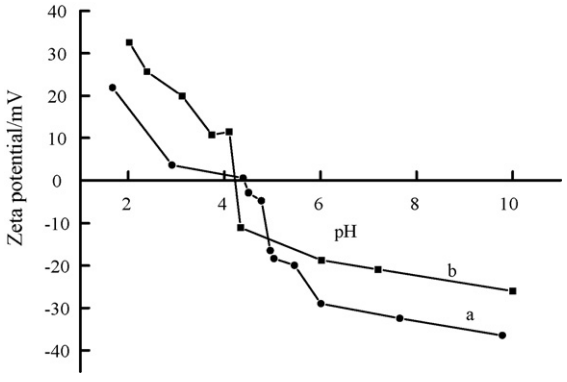

Fig. 10. Plots of the zeta potential as a function of pH for (a) 0.1 g/L AgBr/TiO_2 suspension in the presence of KNO_3 (10^{-3} M) and (b) 0.1 g/L AgBr/TiO_2 suspension in the presence of KNO_3 (10^{-3} M) and $Ni(NO_3)_2$ (5 μM).

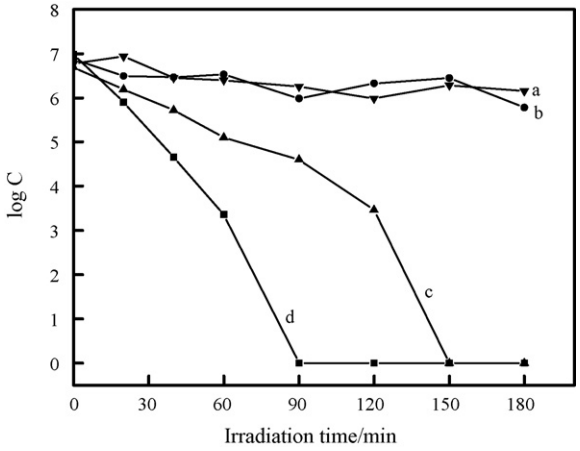

Fig. 12. Temporal course of the bacteria inactivation (2×10^7 cfu/mL, 30 mL) over different catalyst fixed on porous nickel under visible light irradiation. (a) *S. aureus* and (b) *E. coli* over P25 TiO_2 film; (c) *E. coli* and (d) *S. aureus* over AgBr/TiO_2 film.

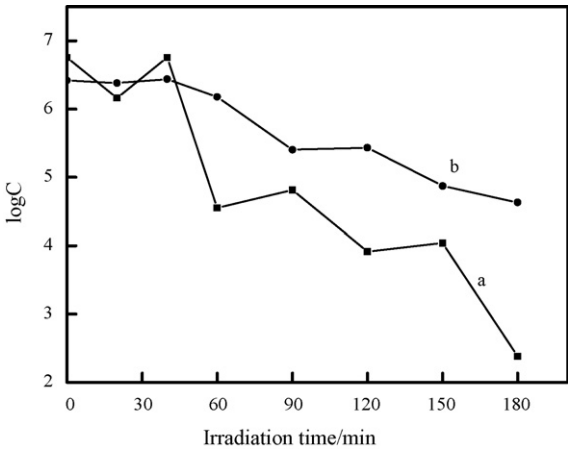

Fig. 13. The inactivation of *E. coli* (~2×10^7 cfu/mL, 30 mL) under weak UV light irradiation (UV-365 intensity = 0.2 mw/cm^2) over different catalyst fixed on porous nickel. (a) AgBr/TiO_2 and (b) P25 TiO_2.

3.5. AgBr/TiO_2 fixed on porous nickel for bacteria inactivation

The photocatalytic inactivation of bacteria over AgBr/TiO_2 immobilized on porous nickel was evaluated. Fig. 12 shows that 6.9 log *E. coli* and *S. aureus* inactivation occurred at 150 and 90 min, respectively, on AgBr/TiO_2 porous nickel film under visible light irradiation. P25 TiO_2 fixed on porous nickel did not show any bactericidal effects under visible light. Meanwhile, under weak UV light irradiation, AgBr/TiO_2 fixed on porous nickel still showed higher activity than fixed P25 TiO_2 (Fig. 13). These results indicated that immobilized AgBr/TiO_2 was a promising material for disinfection.

4. Conclusions

AgBr/TiO_2 showed high visible light-driven bactericidal activity and stability. Furthermore, TEM and K^+ leakage measurement confirmed that the cell wall and cell membrane of pathogenic bacteria were successively destroyed by active species. The interaction between bacteria and AgBr/TiO_2 played an important role in the photocatalytic inactivation of bacteria. In addition, fixed AgBr/TiO_2 showed higher bactericidal activity both under visible and near UV irradiation compared to immobilized P25 TiO_2. The results revealed that AgBr/TiO_2 would be very promising for practical application.

Acknowledgments

This work was supported by the Natural Science Foundation of China (Nos. 20577062, 50621804, 20377050 and 20537020) and the National 863 project of China (Grant No. 2006AA062304).

References

[1] S.D. Richardson, Trends Anal. Chem. 22 (2003) 666.
[2] T. Matsunaga, R. Tomada, T. Nakajima, H. Wake, FEMS Microbiol. Lett. 29 (1985) 211.
[3] P.-C. Maness, S. Smolinski, D.M. Blake, Z. Huang, E.J. Wolfrum, W.A. Jacoby, Appl. Environ. Microbiol. 65 (1999) 4094.
[4] Z. Huang, P.-C. Maness, D.M. Blake, E.J. Wolfrum, S.L. Smolinski, W.A. Jacoby, J. Photochem. Photobiol. A: Chem. 130 (2000) 163.
[5] R.J. Watts, S. Kong, M.P. Orr, G.C. Miller, B.E. Henry, Water Res. 29 (1995) 95.
[6] S. Lee, M. Nakamura, S. Ohgaki, J. Environ. Sci. Health A 33 (1998) 1643.
[7] Y. Kikuchi, K. Sunada, T. Iyoda, K. Hashimoto, A. Fujishima, J. Photochem. Photobiol. A: Chem. 106 (1997) 51.
[8] W. Choi, A. Termin, M.R. Hoffmann, J. Phys. Chem. 98 (1994) 13669.
[9] R. Asahi, T. Morikawa, T. Ohwaki, K. Aoki, Y. Taga, Science 293 (2001) 269.
[10] W. Zhao, W. Ma, C. Chen, J. Zhao, Z. Shuai, J. Am. Chem. Soc. 126 (2004) 4782.
[11] M.D. Driessen, V.H. Grassian, J. Phys. Chem. B 102 (1998) 1418.
[12] E. Bae, W. Coi, Environ. Sci. Technol. 37 (2003) 147.
[13] W. Zhao, C. Chen, X. Li, J. Zhao, J. Phys. Chem. B 106 (2002) 5022.
[14] R.W. Fessenden, P.V. Kamat, J. Phys. Chem. 99 (1995) 12902.
[15] J.M. Stipkala, F.N. Castellano, T.A. Heimer, C.A. Kelly, K.J.T. Livi, G.J. Meyer, Chem. Mater. 9 (1997) 2341.
[16] N. Kakuta, N. Goto, H. Ohkita, T. Mizushima, J. Phys. Chem. B 103 (1999) 5917.
[17] S. Rodrigues, S. Uma, I.N. Martyanov, K.J. Klabunde, J. Catal. 233 (2005) 405.
[18] C. Hu, Y. Lan, J. Qu, X. Hu, A. Wang, J. Phys. Chem. B 110 (2006) 4066.
[19] H. Bader, V. Sturzenegger, J. Hoigne, Water Res. 22 (1988) 1109.
[20] P. Shen, X. Fan, G. Li, Wei Sheng Wu Xue Shiyan, High Education Publisher, Beijing, 2004.
[21] G. Tortora, R.B. Funke, L.C. Case, Microbiology: An Introduction, Addison-Wesley Longman, Inc., New York, 2001.
[22] D.B. Willis, H.L. Ennis, J. Bacteriol. 96 (1968) 2035.
[23] H.L. Ennis, Arch. Biochem. Biophys. 143 (1971) 190.
[24] W.A. Jacoby, P.C. Maness, E.J. Wolfrum, D.M. Blake, J.A. Fennell, Environ. Sci. Technol. 32 (1998) 2650.
[25] C. Hu, X. Hu, L. Wang, J. Qu, A. Wang, Environ. Sci. Technol. 40 (2006) 7903.
[26] C. Hu, J.C. Y, Z. Hao, P.K. Wong, Appl. Catal. B: Environ. 46 (2003) 35.
[27] A.G. Rincon, C. Pulgarin, Appl. Catal. B: Environ. 51 (2004) 283.